RESEARCH ARTICLE

Hermite-Gaussian laser modulation for optimal THz emission in collisional homogeneous plasma

Hitesh Kumar Midha[1] · Vivek Sharma[1] · Niti Kant[2] · Vishal Thakur[1]

Abstract Terahertz (THz) research has gained prominence because to its diverse practical applications in areas including early cancer detection, oral tissue detection, concealed objects detection, food safety and quality inspection, bacteria detection and burn diagnosis. Several efforts have been made to create a customizable and energy-efficient terahertz (THz) generator. This study examines the concurrent transmission of two Hermite-Gaussian (HG) laser pulses in a collisional homogeneous plasma medium. Laser-plasma interaction exhibits nonlinear characteristics, leading to the production of extremely effective THz radiation. An in-depth investigation is conducted to study the relationship between the efficiency of converting terahertz (THz) waves and various parameters such as plasma frequency, Hermite polynomial mode index (s), and electron collisional frequency. Deviation from the resonant direction leads to a decrease in the efficiency of converting THz waves. Efficiency drops to almost zero when the normalized THz frequency surpasses 1.8 and the normalized collisional frequency goes above 4. This study achieves normalised THz amplitude nearly 0.9 and 0.15 for normalised THz frequency and normalised collisional frequency, respectively. Conversion efficiency in the terahertz band increases with higher Hermite polynomial mode index values for s = 0,1,2. The suggested method efficiently produces powerful, customizable, and energy-saving THz radiation by controlling the Hermite polynomial mode index values.

Introduction

THz waves are electromagnetic signals in the frequency range of 0.1 to 10 THz that are non-invasive and non-ionizing. THz waves are used for various diagnostic applications such as early cancer detection, oral tissue detection, concealed objects detection, food safety and quality inspection, bacteria detection and burn diagnosis [1–5]. The interaction between laser and plasma is a significant phenomenon used in generating terahertz (THz) waves, Wakefield acceleration [6, 7], self-focusing and defocusing, harmonics generation, and fusion research [8–19]. Scholars and scientists have analyzed the generation of THz waves through theoretical and experimental methods [20–28]. Sharma et al. [29] researched the Hermite-Gaussian laser pulse in a uniform plasma within the context of laser wakefield acceleration in low-density collisionless plasma. The theoretical research revealed a higher energy gain for mode indices s = 0 and s = 2 compared to s = 1. They analyze the electron energy increase based on pulse duration, plasma density, and beam width for a certain mode index. Pramanik et al. [30] researched the use of a radially polarized Hermite-cosh-Gaussian laser beam for accelerating electrons in an ion channel. They analyzed the relationship between electron energy gain and intensity parameter, laser spot size, decentered parameter, and ion density.

Verma et al. [31] researched the interaction of an electron Bernstein wave with a Hermite-cosh-Gaussian laser beam in a collisional plasma under the influence of a static magnetic field. The researchers visually confirmed that the nonlinear

✉ Vishal Thakur
vishal20india@yahoo.co.in

1 Department of Physics, Lovely Professional University, G.T. Road, Phagwara, Punjab 144411, India

2 Department of Physics, University of Allahabad, Prayag Raj, Uttar Pradesh, India

absorption coefficient is influenced by the Hermite mode index, laser beam width, and decentered parameter.

Tian et al. [32] researched the Hermite-cosh-Gaussian laser beam in inhomogeneous plasma by employing high-order paraxial theory and WKB approximation to analyze self-focusing filamentation instability. The researchers noted that the higher order mode index has a considerable impact on filamentation instability. Ghotra et al. [33] researched the Hermite-cosh-Gaussian laser pulse in low-order axisymmetric modes in a vacuum for electron acceleration. Pandari et al. [34] conducted simulation research on THz generation via femtosecond laser wakefield acceleration in a helium gas jet. Frolov [35] researched the production of THz waves using ultra-short tightly concentrated p-polarized laser pulses on a near-critical plasma slab. The THz wave signal and conversion rate occur at almost normal incidence, as demonstrated by him. Varaki et al. [36] analyze the theoretical aspects of THz wave generation from Wakefield-driven collisional plasma using a skew-cosh-Gaussian laser beam in the presence of an undulator magnetic field. He demonstrates that a low collisional frequency significantly affects Wakefield amplitudes. When the collisional frequency matches the plasma frequency, the amplitude of the Wakefield is reduced. Ashish et al. [37] researched the creation of THz radiation from the interaction of a modulated laser field with plasma in the presence of an axially magnetic field. greater THz field strength is achieved with greater values of mode index.

Zare et al. [38] theoretically analyze the localization of Gaussian beams in hot quantum plasma with a density ramp. An experiment was conducted to study how varying laser intensity affects the critical normalized beam radius at different Fermi temperatures. Punia et al. [39] researched the skew-cosh Gaussian beam in spherical and cylindrical nanoparticles to create a tunable THz radiation source. They demonstrate a shift in the resonance peak towards higher frequencies. Khandale et al. [40] investigated the skew-cosh-Gaussian laser beam in collisional plasma using the Akhmanov parabolic wave equation and paraxial approximation. The study demonstrated that the skewness parameter has a considerable impact on the self-focusing and defocusing of a laser beam.

Two Hermite Gaussian (HG) lasers with radial polarization are moving in the z direction and interacting with a homogenous plasma in this study. The laser beams are characterized by frequencies ω_1 and ω_2, and wave numbers $\vec{k}_1, \vec{k}_2$. By solving the equations of motion, continuity, and Poisson, we derive a non-linear current density. THz fields are generated due to the presence of a non-linear current density. This investigation considers the impact of electron collision. Section II presents the mathematical derivation of the ponderomotive force, the nonlinear plasma current density, and the creation of THz fields.

This is achieved through the examination of the interaction between high-energy laser pulses and an inclined plasma profile. Section III examines the relationship between the normalized THz electric field and the beat frequency, as well as the collisional frequency normalized with the plasma frequency. Section IV presents the ultimate conclusions and results. Citations are provided at the conclusion of the document.

Investigation of THz generation via analytical study

Two Hermite-Gaussian laser beams with radial polarization are propagating in the z-direction and interacting with a homogenous plasma of density n_0. The equations given represent the electric and magnetic fields of laser pulses.

$$\vec{E}_j(r, z) = \hat{r} E_0 H_s\left(\frac{\sqrt{2}r}{r_0}\right) e^{-\left(\frac{r^2}{r_0^2}\right)} e^{i(k_J z - \omega_J t)} \tag{1}$$

$$\vec{B}_j(r, z) = \frac{\left\{\vec{k}_J \times \vec{E}_J(r,z)\right\}}{\omega_J} \quad \text{where} \, J = 1, 2 \tag{2}$$

here, $\vec{B}_j(r, z)$ represents the magnetic field of laser pulse, $r = r(x, y) = \sqrt{x^2 + y^2}$ is radius of Gaussian pulse, r_0 is pulse waist which is a transverse distance where electric field remains 1/e times its value at axis, E_0 is amplitude of laser pulse and s is the mode index of Hermite polynomial H_s.

Hermite functions are defined as follows: $H_0(x) = 1, H_1(x) = 2x, H_2(x) = 4x^2 - 2$. The outcome is dependent on the value of x.

Electrons at rest do not experience any magnetic force in the initial stage. Laser pulses induce oscillatory velocity in plasma electrons as they pass through the plasma.

By employing the equation of motion $md\vec{V}_j/dt = -e\vec{E}_j - m\gamma_{en}\vec{V}_j$ where γ_{en}, e and m represent collision frequency, charge of plasma electron and rest mass, respectively. We determine the velocity of plasma electrons as

$$\vec{V}_j = \frac{e\vec{E}_j}{m(i\omega_J - \gamma_{en})} \tag{3}$$

The oscillating velocity results in a nonlinear ponderomotive force. This force can be defined as

$$\vec{F}_P^{NL} = -\frac{m}{2}\vec{\nabla}\left(\vec{V}_1 . \vec{V}_2^*\right)$$

so, we get

$$\Rightarrow \overrightarrow{F}_P^{NL} = \overrightarrow{F}_{or}^{NL} e^{i((k_1-k_2)z-(\omega_1-\omega_2)t)} = \overrightarrow{F}_{or}^{NL} e^{i(k\prime z-\omega\prime t)} \qquad (4)$$

$$\text{where} \Delta = \left. E_0{}^2 e^2 H_s\left(\frac{\sqrt{2}r}{r_0}\right) e^{-\left(\frac{2r^2}{r_0{}^2}\right)} e^{i(k\prime z-\omega\prime t)} \middle/ \left[2m(i\omega_1-\gamma_{en})(i\omega_2+\gamma_{en})\right] \right. \qquad (4a)$$

$$k\prime = \left(k_1 - k_2\right), \omega\prime = (\omega_1 - \omega_2), \qquad (4b)$$

and

$$\overrightarrow{F}_{or}^{NL} = \Delta\left[\hat{r}\left\{s\left(\frac{4\sqrt{2}r}{r_0}\right)H_{s-1}\left(\frac{\sqrt{2}r}{r_0}\right) + \left(\frac{2b}{r_0}\right)H_s\left(\frac{\sqrt{2}r}{r_0}\right) - \left(\frac{4r}{r_0{}^2}\right)H_s\left(\frac{\sqrt{2}r}{r_0}\right)\right\} + \left\{\hat{z}ik\prime H_s\left(\frac{\sqrt{2}r}{r_0}\right)\right\}\right] \qquad (4c)$$

By solving the equation of motion, $\partial\overrightarrow{V}_{\omega\prime}^{NL}/\partial t = \left(\overrightarrow{F}_P^{NL}/m\right) - \nu_{en}\overrightarrow{V}_{\omega\prime}^{NL}$ and the equation of continuity $\partial n_{\omega\prime}^{NL}/\partial t + \overrightarrow{\nabla}.n\overrightarrow{V}_{\omega\prime}^{NL} = 0$, the value of $\overrightarrow{V}_{\omega\prime}^{NL}$ can be determined.

The plasma density profile is homogeneous with $n = n_0$ where, n_0 represents the initial unperturbed plasma density.

The equation given produces both nonlinear oscillatory velocity and nonlinear density perturbation of plasma electrons.

$$\Rightarrow \overrightarrow{V}_{\omega\prime}^{NL} = \frac{i\omega\prime \overrightarrow{F}_P^{NL}}{m\left(\omega\prime^2 + i\omega\prime\gamma_{en}\right)} \qquad (5)$$

$$\Rightarrow n_{\omega\prime}^{NL} = \frac{n_0 \overrightarrow{\nabla}.\overrightarrow{F}_P^{NL}}{m\left(\omega\prime^2 + i\omega\prime\gamma_{en}\right)} \qquad (6)$$

In this derivation, we assume the value of n remains constant throughout time and is solely dependent on z.

$$\partial(n)/\partial t = 0.$$

Nonlinear density perturbations $n_{\omega\prime}^{NL}$ lead to the creation of a self-consistent space charge potential and field by causing electrons to separate from ions.

This gives rise to linear density perturbation as $n_{\omega\prime}^L = -\chi_P\overrightarrow{\nabla}.(\overrightarrow{\nabla}\phi)/4\pi e$ where, χ_P represents the electric susceptibility of collisional plasma and is calculated as $-\omega_P^2/\left(\omega\prime^2+i\omega\prime\gamma_{en}-k\prime^2 V_{th}^2\right)$.

The Poisson's equation $\nabla^2\phi = 4\pi\left(n_{\omega\prime}^L + n_{\omega\prime}^{NL}\right)e$, is used to calculate the space charge field's linear force, represented as $\overrightarrow{F}_P^L$, acting on the electrons such as

$$\overrightarrow{F}_P^L = e\overrightarrow{\nabla}\phi = \frac{\omega_P^2\overrightarrow{F}_P^{NL}}{\left(1 + \chi_P\right)\left(\omega\prime^2 + i\omega\prime\gamma_{en}\right)} \qquad (7)$$

as, $\omega_P = \sqrt{\left(4\pi n_0 e^2/m\right)}$ is plasma frequency.

To get the nonlinear oscillatory velocity of electrons, one can calculate the equation of motion $\partial\overrightarrow{V}^{NL}/\partial t = \left(\overrightarrow{F}_P^{NL}+\overrightarrow{F}_P^L\right)/m - \gamma_{en}\overrightarrow{V}^{NL}$, which consider the influence of both linear and nonlinear ponderomotive forces.

$$\Rightarrow \overrightarrow{V}^{NL} = \frac{1}{m}\left\{\frac{\omega\prime^2 + i\omega\prime\gamma_{en} - \omega_P^2 + \omega_P^2}{\left(-i\omega\prime + \gamma_{en}\right)\left(\omega\prime^2 + i\omega\prime\gamma_{en} - \omega_P^2\right)}\right\}\overrightarrow{F}_P^{NL} \qquad (8)$$

Nonlinear oscillatory current density is shows as

$$\overrightarrow{J}^{NL} = -\frac{1}{2}n_0 e\overrightarrow{V}^{NL}$$
$$= -\frac{n_0 e}{2m}\left\{\frac{\omega^2 + i\omega\gamma_{en} - \omega_P^2 + \omega_P^2}{\left(-i\omega + \gamma_{en}\right)\left(\omega\prime^2 + i\omega\gamma_{en} - \omega_P^2\right)}\right\}\overrightarrow{F}_{or}^{NL} e^{i(kz-\omega t)} \qquad (9)$$

where, $\left(k_1 - k_2\right) = k \approx k\prime$, $\left(\omega_1 - \omega_2\right) = \omega \approx \omega\prime$.

k and ω denote the propagation constant and frequency of the terahertz (THz) field, respectively. The vector $\overrightarrow{J}^{NL}$ results in the production of THz fields.

By solving Maxwell's equations $\overrightarrow{\nabla} \times \overrightarrow{E} = -\frac{1}{c}\left(\partial\overrightarrow{B}/\partial t\right)$ and $\overrightarrow{\nabla} \times \overrightarrow{B} = \frac{\varepsilon}{c}\left(\partial\overrightarrow{E}/\partial t\right) + \frac{4\pi}{c}\overrightarrow{J}^{NL}$

The equation for generating terahertz waves is as follows.

$$\Rightarrow \overrightarrow{\nabla}.\left(\overrightarrow{\nabla}.\overrightarrow{E}_{THz}\right) - \nabla^2\overrightarrow{E}_{THz} = \frac{\omega^2}{c^2}\varepsilon\overrightarrow{E}_{THz} + \frac{4\pi i\omega}{c^2}\overrightarrow{J}^{NL} \qquad (10)$$

The symbol $\overrightarrow{E}_{THz}$ denotes the electric field of the produced THz pulse.

Here, we ignore the higher order derivatives due to the frequent variations in the THz field.

here, the expression expresses the electrical permittivity of collisional plasma as

$$\varepsilon = 1 - \left[\omega_P^2 \middle/ \left\{ \omega^2 + i\omega\gamma_{en} \right\} \right].$$

For the Solution of Eq. (10), we utilize the nonlinear oscillatory current density value from Eq. (9) along with the ε value to determine the normalized amplitude of the THz field. We are examining the electric field component along the radial direction.

$$\frac{E_{THz}}{E} = \frac{i\omega_P^2}{\varepsilon\omega} \frac{e}{2r_0} \left\{ \frac{\omega^2 + i\omega\gamma_{en} - \omega_P^2 + \omega_P^2}{(-i\omega + \gamma_{en})(\omega^2 + i\omega\gamma_{en} - \omega_P^2)} \right\} \frac{E_0 H_s\left(\frac{\sqrt{2}r}{r_0}\right) e^{-\left(r^2 \middle/ r_0^2\right)}}{2m(i\omega_1 - \gamma_{en})(i\omega_2 + \gamma_{en})}$$
$$\left[\hat{r} \left\{ s\left(4\sqrt{2}\right) H_{s-1}\left(\frac{\sqrt{2}r}{r_0}\right) + (2b) H_s\left(\frac{\sqrt{2}r}{r_0}\right) - \left(\frac{4r}{r_0}\right) H_s\left(\frac{\sqrt{2}r}{r_0}\right) \right\} \right]$$
(11)

The ratio, $\frac{E_{THz}}{E}$ represents the relationship between the generated THz electric field and the applied laser electric field. This ratio is known as THz conversion efficiency.

Result and discussion

The study examines the generation of terahertz (THz) radiation by HG laser pulses interacting in a collisional plasma. The plasma density is $9.74 \times 10^{22} m^{-3}$, and the related plasma frequency is 1.76×10^{13} Hz. The frequencies of the CO_2 laser are $\omega_1 = 1.973 \times 10^{14} \text{rad/s}$ and $\omega_2 = 1.783 \times 10^{14} \text{rad/s}$, both exceeding ω_P. The laser pulses have wavelengths of $\lambda_1 = 9.57 \mu m$ and $\lambda_2 = 10.57 \mu m$. The Gaussian laser beam waist is $r_0 = 5 \times 10^{-5}$ m, and the amplitude of the laser field is $E_0 = 2 \times 10^{11} V/m$.

Effect of laser frequency

This section examines the change in normalized THz amplitude at various normalized THz frequencies. Curves are graphed for various values of s = 0, 1 and 2 with a collisional frequency γ_{en} of $0.1\omega_P$. The graphs are displayed in Fig. 1a, b, and c. Figure 1d displays the comparative graph.

The normalized amplitude of THz waves grows as the Hermite polynomial mode index value (s = 0,1,2) increases. At resonance ($\omega = \omega_P$), the normalized THz amplitude reaches its peak. When the ratio of ω/ω_P exceeds one, the amplitude of THz diminishes and tends towards zero for values of ω/ω_P

greater than 1.8. The normalized amplitude of THz waves is approximately 0.08 and 0.25 for Hermite polynomial mode indices s = 0 and 1, and it approaches to 0.9 for s = 2.

The Hermite mode index quantifies the spatial distribution of the laser beam's intensity profile. Various Hermite modes have distinct spatial distributions. The selection of the mode has an impact on the spatial distribution of laser energy, which subsequently impacts the dynamics of the plasma and the formation of THz waves. Same can be seen in the theoretical study of this study.

Effect of collision frequency (γ_{en})

This section examines the change in normalized THz amplitude at various normalized collisional frequencies. We have plotted curves for s values of 0, 1, and 2 at a THz frequency of $\omega = 1.9 \times 10^{13}$ Hz, depicted in Fig. 2a, b, and c. Figure 2d displays the comparative graph.

Normalized terahertz amplitude rises with the increase in Hermite polynomial mode index value (s = 0,1,2). At resonance ($\omega = \omega_P$), the normalized THz amplitude reaches its peak. When the value of γ_{en}/ω_P exceeds one, the THz amplitude declines and tends towards zero for γ_{en}/ω_P values greater than four. The normalized amplitude of the THz signal is around 0.012 and 0.04 for Hermite polynomial modes with index s = 0 and 1 and increases to 0.15 for s = 2. The Hermite polynomial undergoes large changes in its values with variations in the s values. A new type of laser electric field is produced, leading to a major impact on THz generation. Similar findings are seen in our analytical data.

Effect of normalized collisional frequency (γ_{en}/w_P) and normalised frequency

The normalized amplitude of THz waves is calculated for various normalized collisional frequency and varied levels of normalised frequency from 0 to 1.30. A 3D curve is presented for Hermite polynomial mode index value s = 1 at $E_0 = 2 \times 10^{11}$ V/m (Fig. 3).

With the Hermite polynomial mode index value s = 1, the normalized collisional frequency and normalized THz amplitude both increase from 0 to more than 0.6 for different values of normalised frequency ranging from zero to 1.30. This study's results show a notable increase in normalized Terahertz (THz) amplitude at resonance conditions, and it reduces significantly and tends to zero in off-resonant conditions.

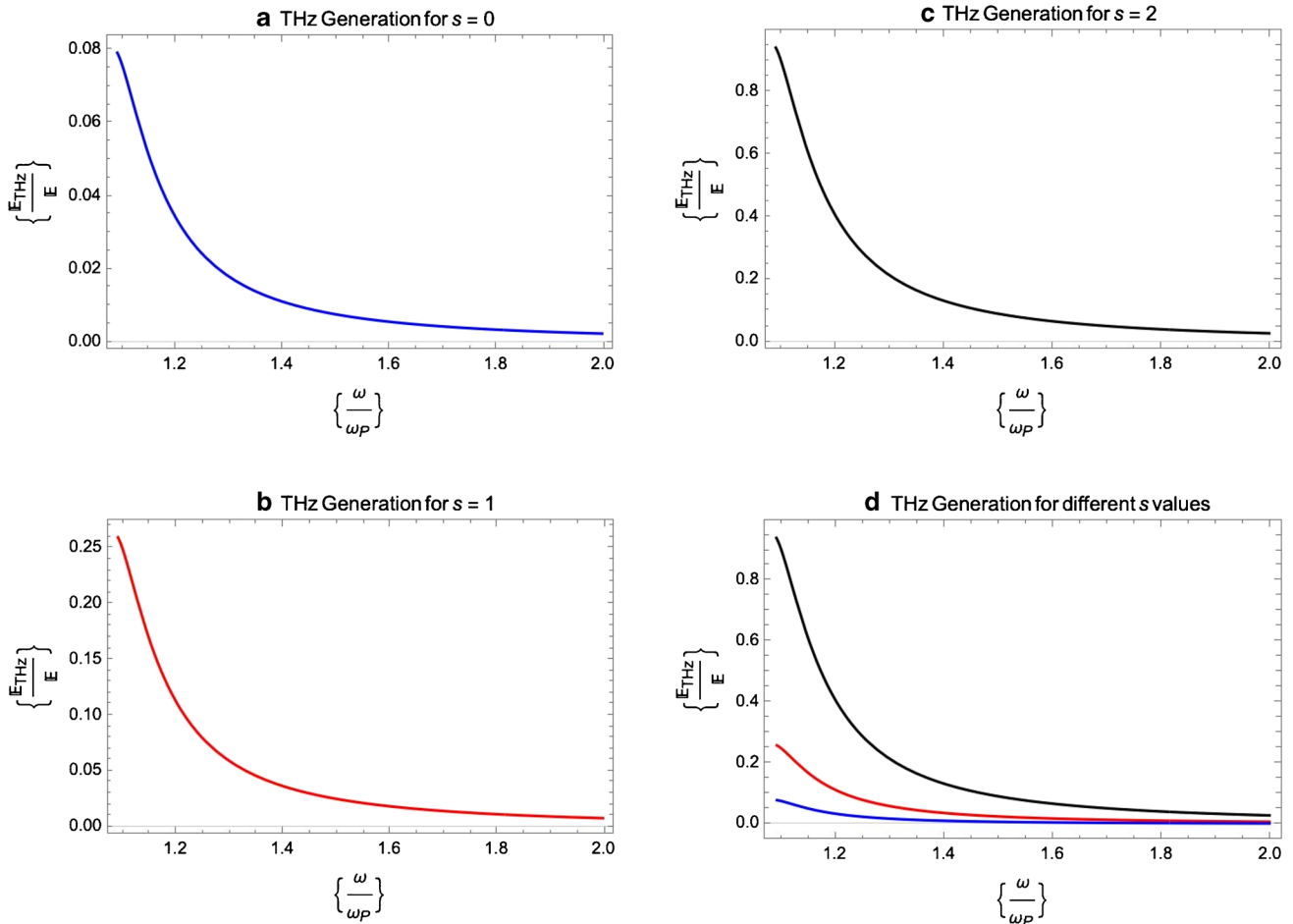At high collisional frequencies, the plasma does not result in an increase in THz generation. The reason for

Fig. 1 a Variation of normalized THz amplitude with normalized THz frequency. For r=0.3r_0 s=0. **b** Variation of normalized THz amplitude with normalized THz frequency. For r=0.3r_0 s=1. **c** Variation of normalized THz amplitude with normalized THz frequency. For r=0.3r_0 s=2. **d** Variation of normalized THz amplitude with normalized THz frequency. For r=0.3r_0, s=0 (blue), 1 (red), 2 (black)

this is because collisional processes have a greater influence than the nonlinear interactions that are responsible for generating THz waves.

This investigation's results are consistent with the findings reported by Choudhary et al. [41]. Researchers have found that using the Hermite-cosh-Gaussian beam is a viable approach for generating terahertz (THz) radiation. We utilized a Hermite-Gaussian beam to generate terahertz (THz) waves in a collisional plasma profile with a homogeneous plasma.

Conclusion

This work examines the propagation of two Hermite-Gaussian laser beams in a collisional homogeneous plasma. The plasma density is constant in the pulse direction. This study generates efficient THz waves through the technique of nonlinear laser plasma interaction. The results analyze the correlation between normalized THz amplitude and normalized THz frequency, as well as collisional frequency, across various Hermite polynomial mode index values (s = 0, 1, 2). As we deviate from resonance, the efficiency of generated THz declines quickly and eventually approaches zero for various values of normalized THz frequency and normalized collisional frequency. The THz conversion efficiency is low, with values of for s = 0 and 1, respectively. It increases significantly for s = 2, reaching 0.9 and 0.15 for normalized THz frequency and normalized collisional frequency, respectively. The THz conversion efficiency increases with higher values of the Hermite polynomial mode index (s = 0, 1, 2). This approach is particularly advantageous for producing an effective, adjustable THz source.
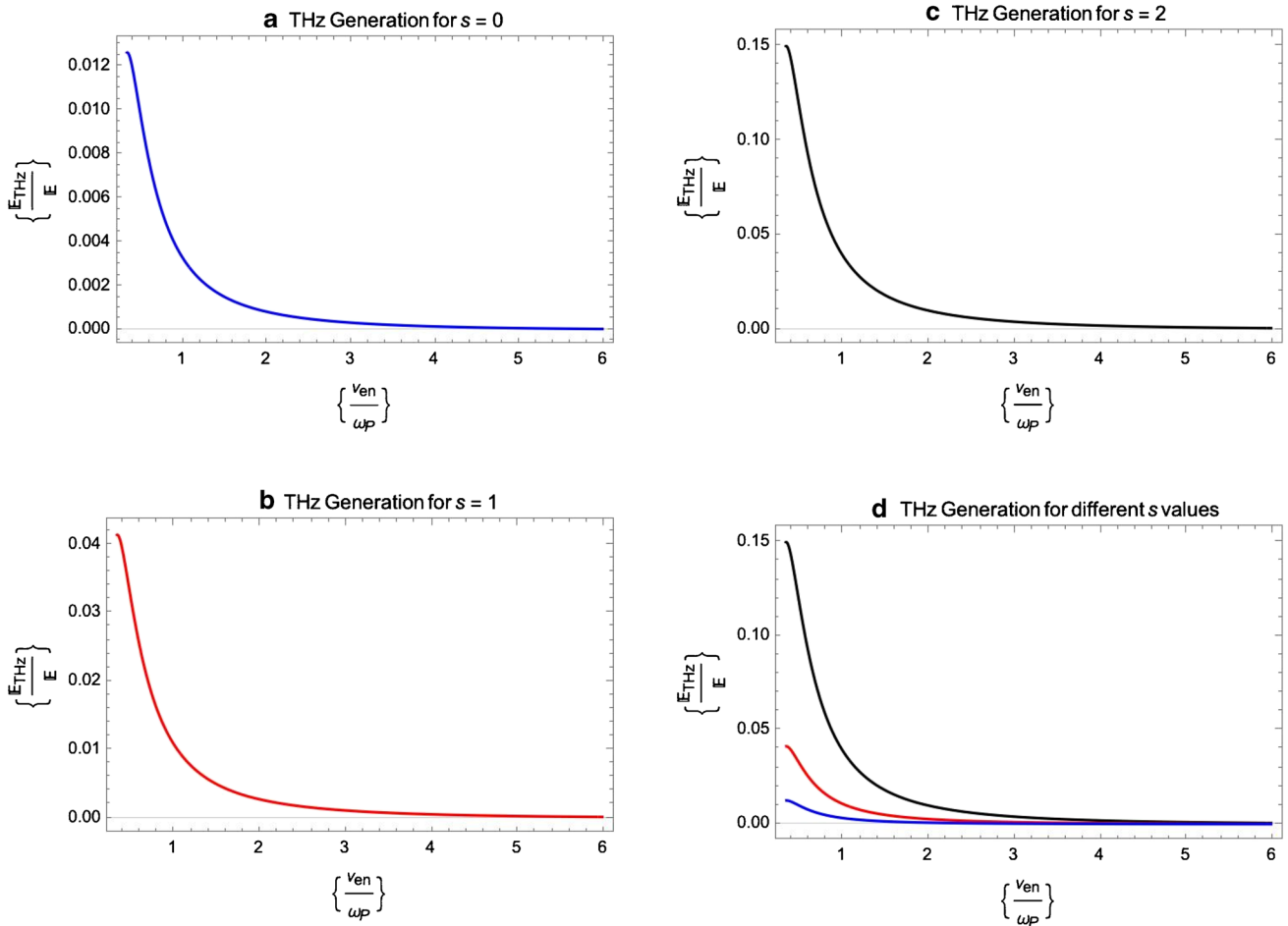
Fig. 2 a Variation of normalized THz amplitude with normalized collisional frequency. For r = 0.3r_0, s = 0. **b** Variation of normalized THz amplitude with normalized collisional frequency. For r = 0.3r_0, s = 1. **c** Variation of normalized THz amplitude with normalized col-

lisional frequency. For r = 0.3r_0, s = 2. **d** Variation of normalized THz amplitude with normalized collisional frequency. For r = 0.3r_0, s = 0 (blue), 1 (red), 2 (black)

Fig. 3 Variation of normalized THz amplitude with normalized collisional frequency and normalised frequency for s=1. Other parameters are same as mentioned above
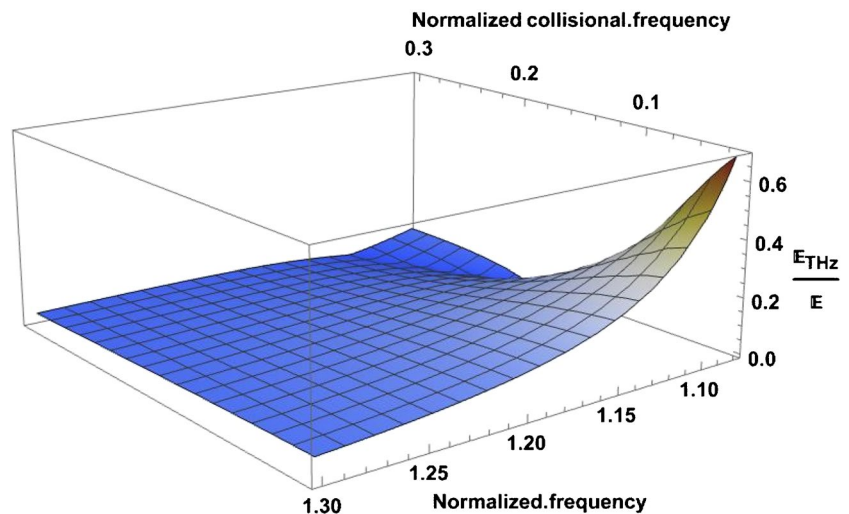
Declarations

Ethics approval Not applicable.

Consent to participate Not applicable.

Consent for publication Not applicable.

Conflict of interest The authors declare no competing interest.

References

1. M.E. Khani, Z.B. Harris, O.B. Osman, A.J. Singer, M.H. Arbab, Triage of in vivo burn injuries and prediction of wound healing outcome using neural networks and modeling of the terahertz permittivity based on the double Debye dielectric parameters. Biomed. Opt. Express **14**(2), 918–931 (2023)

2. Z. Ma et al., Identification and quantitative detection of two pathogenic bacteria based on a terahertz metasensor. Nanoscale **15**(2), 515–521 (2023)

3. R. Cheng, S. Lucyszyn, Few-shot concealed object detection in sub-THz security images using improved pseudo-annotations. Sci. Rep. **14**(1), 3150 (2024)

4. H. Ge et al., Tri-band and high FOM THz metamaterial absorber for food/agricultural safety sensing applications. Opt. Commun. **554**, 130173 (2024)

5. S. Yang et al., Studying oral tissue via real-time high-resolution terahertz spectroscopic imaging. Phys. Rev. Appl. **19**(3), 34033 (2023)

6. V. Sharma, V. Thakur, Analyzing electron acceleration mechanisms in magnetized plasma using Sinh–Gaussian pulse excitation. J. Opt. (2024). https://doi.org/10.1007/s12596-024-01709-0

7. V. Sharma, V. Thakur, A comprehensive study of magnetic field-induced modifications in sin-Gaussian pulse-driven laser wakefield acceleration. J. Opt. (2024). https://doi.org/10.1007/s12596-023-01636-6

8. X. Xie, J. Dai, X.-C. Zhang, Coherent control of THz wave generation in ambient air. Phys. Rev. Lett. **96**(7), 075005 (2006)

9. Z. Hu, Z. Sheng, W. Ding, W. Wang, Q. Dong, J. Zhang, Electromagnetic emission from laser wakefields in magnetized underdense plasmas. Plasma Sci. Technol. **14**(10), 874–879 (2012)

10. Z.M. Sheng, K. Mima, J. Zhang, H. Sanuki, Emission of electromagnetic pulses from laser wakefields through linear mode conversion. Phys. Rev. Lett. **94**(9), 095003 (2005)

11. T. Tajima, X.Q. Yan, T. Ebisuzaki, Wakefield acceleration. Rev. Mod. Plasma Phys. **4**(1), 7 (2020)

12. E. Gschwendtner, P. Muggli, Plasma wakefield accelerators. Nat. Rev. Phys. **1**(4), 246–248 (2019)

13. F. Osman, R. Castillo, H. Hora, Relativistic and ponderomotive self-focusing at laser–plasma interaction. J. Plasma Phys. **61**(2), 263–273 (1999)

14. H. Hora, Theory of relativistic self-focusing of laser radiation in plasmas. J. Opt. Soc. Am. **65**(8), 882 (1975)

15. B. Ritchie, Relativistic self-focusing and channel formation in laser-plasma interactions. Phys. Rev. E **50**(2), R687–R689 (1994)

16. M.V. Takale, S.T. Navare, S.D. Patil, V.J. Fulari, M.B. Dongare, Self-focusing and defocusing of TEM0p Hermite-Gaussian laser beams in collisionless plasma. Opt. Commun. **282**(15), 3157–3162 (2009)

17. U. Teubner, P. Gibbon, High-order harmonics from laser-irradiated plasma surfaces. Rev. Mod. Phys. **81**(2), 445–479 (2009)

18. L. Fedeli, A. Formenti, L. Cialfi, A. Sgattoni, G. Cantono, M. Passoni, Structured targets for advanced laser-driven sources. Plasma Phys. Control. Fusion **60**(1), 014013 (2018)

19. G.Q. Liao et al., Intense terahertz radiation from relativistic laser-plasma interactions. Plasma Phys. Control. Fusion **59**(1), 014039 (2017)

20. F. Jahangiri, M. Hashida, T. Nagashima, S. Tokita, M. Hangyo, S. Sakabe, Intense terahertz emission from atomic cluster plasma produced by intense femtosecond laser pulses. Appl. Phys. Lett. **99**(26), 261503 (2011)

21. F. Bakhtiari, M. Esmaeilzadeh, B. Ghafary, Terahertz radiation with high power and high efficiency in a magnetized plasma. Phys. Plasmas **24**(7), 073112 (2017)

22. J.A. Fülöp, Z. Ollmann, Cs. Lombosi, C. Skrobol, L. Klingebiel, L. Pálfalvi, F. Krausz, S. Karsch, J. Hebling et al., Efficient generation of THz pulses with 0.4 mJ energy. Opt. Express **22**, 20155–20163 (2014)

23. A. Gopal et al., Characterization of 700 μJ T rays generated during high-power laser solid interaction. Opt. Lett. **38**(22), 4705 (2013)

24. K.Y. Kim, A.J. Taylor, J.H. Glownia, G. Rodriguez, Coherent control of terahertz supercontinuum generation in ultrafast laser-gas interactions. Nat. Photon. **2**(10), 605–609 (2008)

25. C. Vicario, A.V. Ovchinnikov, S.I. Ashitkov, M.B. Agranat, V.E. Fortov, C.P. Hauri, Generation of 09-mJ THz pulses in DSTMS pumped by a Cr:Mg_2SiO_4 laser. Opt. Lett. **39**(23), 6632 (2014)

26. H. Hamster, A. Sullivan, S. Gordon, R.W. Falcone, Short-pulse terahertz radiation from high-intensity-laser-produced plasmas. Phys. Rev. E **49**(1), 671–677 (1994)

27. H.C. Wu, Z.M. Sheng, J. Zhang, Single-cycle powerful megawatt to gigawatt terahertz pulse radiated from a wavelength-scale plasma oscillator. Phys. Rev. E Stat. Nonlin. Soft Matter Phys. **77**(4), 046405 (2008)

28. H.B. Zhuo et al., Terahertz generation from laser-driven ultrafast current propagation along a wire target. Phys. Rev. E **95**(1), 13201 (2017)

29. V. Sharma, V. Thakur, Enhanced laser wakefield acceleration utilizing Hermite-Gaussian laser pulses in homogeneous plasma. J Opt (2023). https://doi.org/10.1007/s12596-023-01565-4

30. A.K. Pramanik, H.S. Ghotra, J. Rajput, Efficient electron acceleration by radially polarized Hermite-Cosh-Gaussian laser beam in an ion channel. Eur. Phys. J. D **77**(8), 161 (2023)

31. A. Varma, S.P. Mishra, A. Kumar, A. Kumar, Electron Bernstein wave aided Hermite cosh-Gaussian laser beam absorption in collisional plasma. Laser Phys. Lett. **20**(7), 76001 (2023)

32. K. Tian, X. Xia, Filamentation instability in the interaction of high-order Hermite cosh Gaussian laser beam and inhomogeneous plasmas. Results Opt. **12**, 100449 (2023)

33. H.S. Ghotra, Electron acceleration by low order axisymmetric modes of Hermite-Cosh-Gaussian laser pulses in vacuum. Phys. Scr. **98**(12), 125602 (2023)

34 M. Rezaei-Pandari et al., Investigation of terahertz radiation generation from laser-wakefield acceleration. AIP Adv. **14**(2), 025347 (2024)

35. A.A. Frolov, Emission of terahertz pulses from near-critical plasma slab under action of p-polarized laser radiation. J. Plasma Phys. **90**(1), 905900116 (2024)

36. M. Abedi-Varaki, THz radiation generation from plasma wakefield driven by skew-cosh-Gaussian laser beam under an undulator magnetic field. Waves in Random and Complex Media , 1–12 (2024)

37. Ashish, K. Gopal, D.N. Gupta, S. Singh, A. Vijay, Terahertz radiation generation from amplitude-modulated laser filament interaction with a magnetized plasma. Modern Physics Letters B **268**, 2450192 (2024)

38. S. Zare, N. Kant, Localization of a Gaussian laser beam in thermal quantum plasma with density ramp. J. Opt. **53**(1), 216–222 (2024)

39. T. Punia, H.K. Malik, Terahertz tuning by core-shell nanoparticles irradiated by skew-cosh Gaussian lasers. Phys. Scr. **99**(3), 35605 (2024)

40. K.Y. Khandale et al., Self-focusing/defocusing of skew-cosh-Gaussian laser beam for collisional plasma. Laser Phys. **34**(3), 36001 (2024)

41. S. Chaudhary, K.P. Singh, U. Verma, A.K. Malik, Radially polarized terahertz (THz) generation by frequency difference of Hermite Cosh Gaussian lasers in hot electron-collisional plasma. Opt. Lasers Eng. **134**, 106257 (2020)